Quantum Monte Carlo using a Stochastic Poisson Solver

D. Das, R. M. Martin, M. H. Kalos

Disclaimer

This document was prepared as an account of work sponsored by an agency of the United States Government. Neither the United States Government nor the University of California nor any of their employees, makes any warranty, express or implied, or assumes any legal liability or responsibility for the accuracy, completeness, or usefulness of any information, apparatus, product, or process disclosed, or represents that its use would not infringe privately owned rights. Reference herein to any specific commercial product, process, or service by trade name, trademark, manufacturer, or otherwise, does not necessarily constitute or imply its endorsement, recommendation, or favoring by the United States Government or the University of California. The views and opinions of authors expressed herein do not necessarily state or reflect those of the United States Government or the University of California, and shall not be used for advertising or product endorsement purposes.

Quantum Monte Carlo using a Stochastic Poisson Solver

Dyutiman Das and Richard M. Martin
University of Illinois at Urbana-Champaign
1110 W. Green St., Urbana, IL 61801

Malvin H. Kalos
Lawrence Livermore National Laboratories
7000 East Ave., Livermore, CA 94550
(Dated: May 4, 2005)

Quantum Monte Carlo (QMC) is an extremely powerful method to treat many-body systems. Usually quantum Monte Carlo has been applied in cases where the interaction potential has a simple analytic form, like the $1/r$ Coulomb potential. However, in a complicated environment as in a semiconductor heterostructure, the evaluation of the interaction itself becomes a non-trivial problem. Obtaining the potential from any grid-based finite-difference method, for every walker and every step is unfeasible. We demonstrate an alternative approach of solving the Poisson equation by a classical Monte Carlo within the overall quantum Monte Carlo scheme. We have developed a modified "Walk On Spheres" algorithm using Green's function techniques, which can efficiently account for the interaction energy of walker configurations, typical of quantum Monte Carlo algorithms. This stochastically obtained potential can be easily incorporated within popular quantum Monte Carlo techniques like variational Monte Carlo (VMC) or diffusion Monte Carlo (DMC). We demonstrate the validity of this method by studying a simple problem, the polarization of a helium atom in the electric field of an infinite capacitor.

I. INTRODUCTION

Simulation of an N-particle quantum system is essentially solving the Schrödinger's equation involving the $3N$-dimensional wave-function which defines the state of the system. Stochastic methods like quantum Monte Carlo (QMC) are very appropriate, useful and accurate to treat systems of such large dimensionality[1,2]. These methods have been applied extensively to study properties like cohesive energies of molecules[3], solids[4], properties of the electron gas[5,6], solid hydrogen[7,8], clusters[9] and much more.

Recently there has been great interest in studying semiconductor devices operating in highly quantum regimes, like quantum dot devices[10], quantum wires[11], single electron transistors[12] etc. For simulation purposes structural details of these devices are usually represented by simple analytically tractable models[13]. However these models sometimes lead to an inadequate description of the interaction energies[14]. There have been only a limited number of applications of quantum Monte Carlo to realistic models of such physical devices capturing the details of the potential profile[15], and even this known work has been restricted to making simplifying assumptions on the form of the potential. The reason is that while simulation of natural or idealized structures involve interactions with simple analytic forms (like Coulomb, Lennard-Jones etc.), the interaction in artificial devices is too complicated to be efficiently treated within quantum Monte Carlo. Our goal is to extend the application of quantum Monte Carlo to semiconductor devices in a simple and straightforward way.

Among the several quantum Monte Carlo methods, we will mainly focus on zero temperature methods like variational Monte Carlo (VMC)[16] and diffusion Monte Carlo (DMC), since these are the simplest to code and most extensively used. We should mention here that our approach can also be used in conjunction with any other kind of quantum or classical Monte Carlo algorithms. The methods we are concerned with, i.e. variational and diffusion Monte Carlo both follow the same basic idea, they calculate expectation of observables associated with a particular state of the system. Consider an N-particle system, and denote the coordinate of the i-th particle by $\boldsymbol{q}_i$. The simulation generates a set of M configurations $\{\boldsymbol{R}\}$, called "walkers".

$$\{\boldsymbol{R}\} = \boldsymbol{R}_1, \ldots, \boldsymbol{R}_m, \ldots, \boldsymbol{R}_M. \quad \boldsymbol{R}_m = \{\boldsymbol{q}_1, \ldots, \boldsymbol{q}_N\} \ \forall \ m,$$

i.e. each walker is a realization of the system in a particular configuration. The algorithm to generate $\{\boldsymbol{R}\}$ depends on the method involved, but it results in the walkers being distributed according to (or something close to) Ψ^2, where Ψ is the relevant state. Accurate estimate of any observable can then be obtained.

Application of these methods to an entire device structure can be prohibitively expensive. Progress can be made by isolating the physical region dominated by quantum mechanics from the background, which can be treated semi-classically. The walkers are created only in the quantum region and are confined there. The potential profile in this region is thus governed by the complicated inter-particle interactions, the effect of the semi-classical background, induced image charges and the gate voltages on the surface boundary of the device. The net effect in general is very complicated.

This potential profile is however the defining characteristic of the system. The quantum Monte Carlo algorithms inevitably involve repeated computation of the potential energy $V(\boldsymbol{R}_m)$ of each walker configuration $\boldsymbol{R}_m$ during and after their evolution into the final equilibrium distribution. In general, there will be no analytic expression for $V(\boldsymbol{R}_m)$ except in highly idealized cases, and will have to be obtained as an explicit solution of Poisson's equation at every step. This is unfeasible for any grid based finite element like method.

The only application[15] of quantum Monte Carlo to realistic devices that we know of, circumvents this by approximating the background potential by a self-consistent Poisson-Schrödinger solution using an LSDA quantum charge density. The walkers move around in this rigid background, and the particles interact by a simple Coulomb interaction. But strictly speaking, the interaction is not Coulomb-like, it is modified by the induced charges at dielectric interfaces and metal surfaces. Also the LSDA approximation itself breaks down for highly correlated systems producing theoretically impossible results like predicting phase transitions in finite systems[17,18]. However, we will show that quantum Monte Carlo can be applied to realistic models of such systems without these approximations, if we can solve the potential stochastically.

Our stochastic approach has several advantages. Traditional grid based methods expend a lot of computation in solving the equation at all grid points over the entire device. These grid points are placed at discrete intervals, and thus limit the resolution of the device structure. This resolution can be increased only at considerable cost. However, the stochastic method obtains the solution only at the desired points (for e.g. the walker configuration $\boldsymbol{R}_m$). Secondly, this does not suffer from the resolution issues of the grid based methods, any point can be treated with arbitrary accuracy. Moreover, the stochastic methods can handle regions of very sharp gradients much more effectively than grid based counterparts.

In this introductory paper we will only present the mechanism of using the stochastic potential solver in conjunction with quantum Monte Carlo. To this end, we will investigate a very simple system with a known analytic potential, to test the applicability of this method. Application to realistic devices will be presented in future work. The rest of the paper is organized as follows. In section II we describe the existing methods of solving Poisson's equation by Monte Carlo. In section III, we adapt this method to account for discrete point charges like walker densities. In section IV, we describe different techniques by which we can greatly increase the efficiency for certain situations. In section V, we incorporate this technique into quantum Monte Carlo and in VI we present a simple calculation of the polarizability of a helium atom in between plates of an infinite capacitor, using variational and diffusion Monte Carlo.

II. STOCHASTIC POTENTIAL SOLVER

The probabilistic potential theory arises from the connection between Brownian motion and classical potential theory, first made by Kakutani in 1944[19]. Interestingly, the first use of Monte Carlo to solve Schrödiger's equation, by Fermi, Metropolis, Ulam et al was also around the same time in 1948[20]. However, Muller[21] was the first to layout a detailed mathematical framework and algorithm to solve Laplace's equation, which was later developed by Haji-Sheikh[22] when he applied this method for a non-zero constant heat-source term. Physically, heat flow, natural diffusion, Brownian motion and potential, all follow similar diffusion equations, and hence can be solved by similar stochastic methods. A nice and more detailed introduction can be found in the work of Bevensee[23].

Of the various stochastic approaches to the potential problem[24], we will present the "Floating Random Walk" algorithm for both its clarity and usefulness for our purpose. The main idea is best illustrated in a charge free system (Laplace's equation), the basic algorithm being same even for the general problem as will be shown in the next section. We know that the solution of Laplace's equation are harmonic functions which obey the Mean Value Theorem[25]

$$\Phi(\boldsymbol{r}) = \frac{1}{4\pi d^2} \int \Phi(\boldsymbol{r}')d^2\boldsymbol{r}', \qquad (1)$$

i.e. the potential $\Phi(\boldsymbol{r})$ at any point $\boldsymbol{r}$ is the average of the potential over a sphere of arbitrary radius d centered at $\boldsymbol{r}$. Here we will use $\boldsymbol{r}$ and $P(\boldsymbol{r})$ interchangeably to denote the same point. We assume Dirichlet boundary conditions, i.e. the potential is known on the external surface. Neumann boundary conditions can also be accommodated[22]. A simple random walk algorithm called "The Walk On Spheres" (WOS) due to Muller[21] can solve Eq.(1) in a very elegant way.

Consider a region Ω with external boundary $\partial\Omega$ where the potential is specified, $\Phi_{\mathrm{app}}(\boldsymbol{r})$ for $\boldsymbol{r} \in \partial\Omega$, see Fig.(1). To obtain the potential at any point $P(\boldsymbol{r} \in \Omega)$, construct the largest possible sphere S_0 centered at $P(\boldsymbol{r})$ but fully contained within Ω. Such constructions will be called the "maximum sphere" following Muller. The radius of this sphere is simply the minimum distance to the boundary $\partial\Omega$. The averaging of Eq.(1) is carried out by sampling points $\boldsymbol{r}_1$ (and the potential $\Phi(\boldsymbol{r}_1)$) uniformly over the surface of S_0. Hence the solution $\Phi(\boldsymbol{r})$, represented by the estimator $\langle\tilde{\Phi}(\boldsymbol{r})\rangle$ is given by $\langle\Phi(\boldsymbol{r}_1)\rangle$. Here $\tilde{\Phi}(\boldsymbol{r})$ is the estimate of an individual sample.

But of course, the potential $\Phi(\boldsymbol{r}_1)$ is unknown, and thus we need to continue the process giving rise to a "walk" as illustrated in Fig.(1). A maximum sphere is constructed centered about $\boldsymbol{r}_1$, and a point $\boldsymbol{r}_2$ is sampled on it, and the walk continues until the sampled point $\boldsymbol{r}^\star$ lies on, or very near the boundary $\partial\Omega$, where the potential is known. $\Phi(\boldsymbol{r}^\star \in \partial\Omega) = \Phi_{\mathrm{app}}(\boldsymbol{r}^\star)$. This generates a walk $\boldsymbol{q} \to \boldsymbol{r}_1 \to \boldsymbol{r}_2 \cdots \boldsymbol{r}^\star$, see Fig.(1). An average over
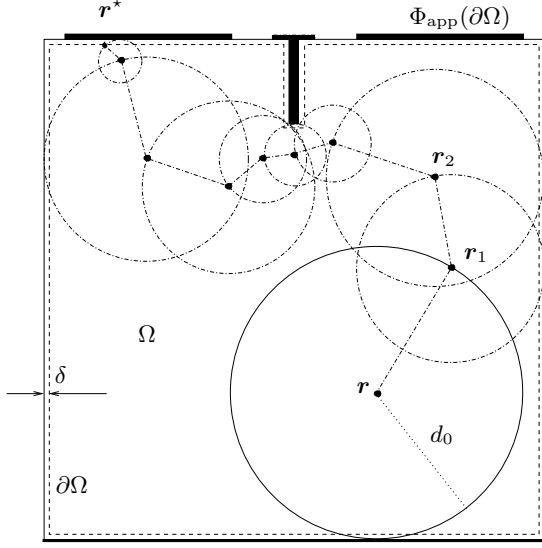
FIG. 1: A Walk On Spheres: A generic device with metal gates on surface held at arbitrary voltages. Start by constructing the maximum sphere S_0 of radius d_0 centered on $P(\boldsymbol{r})$. Sample a point $\boldsymbol{r}_1$ uniformly on S_0. Repeat the process by constructing sphere S_1 etc. The walk ends when the sampled point $\boldsymbol{r}^\star$ is within a range δ of boundary $\partial\Omega$. Such walks will never end exactly on the boundary, but with $\delta \ll d_0$ the estimate can be made arbitrarily accurate.

many such walks will provide an estimate of the potential at $P(\boldsymbol{r})$, the starting point. Hence, $\langle \tilde{\Phi}(\boldsymbol{r}) \rangle = \langle \Phi_{\text{app}}(\boldsymbol{r}^\star) \rangle$. Thus, for $\mathcal{N}$ such walks the mean of the estimate is

$$\langle \tilde{\Phi}(\boldsymbol{r}) \rangle = \lim_{\mathcal{N} \to \infty} \frac{1}{\mathcal{N}} \sum_{n=1}^{\mathcal{N}} \Phi_{\text{app}}(\boldsymbol{r}_n^\star),$$

with an error of

$$\delta \tilde{\Phi}(\boldsymbol{r}) = \lim_{\mathcal{N} \to \infty} \frac{1}{\mathcal{N}-1} \left[\frac{1}{\mathcal{N}} \sum_{n=1}^{\mathcal{N}} \Phi_{\text{app}}^2(\boldsymbol{r}_n^\star) - \langle \tilde{\Phi}(\boldsymbol{r}) \rangle^2 \right].$$

III. THE GREEN'S FUNCTION APPROACH

Much insight into the above method can be obtained from a full mathematical treatment of the general problem, namely the Poisson's equation

$$\nabla^2 \Phi(\boldsymbol{r}) = -\rho(\boldsymbol{r})/\varepsilon \tag{2}$$

where $\rho(\boldsymbol{r})$ is the charge density, and ε is the dielectric constant of the medium. Keeping in mind the discrete nature of walker configurations in quantum Monte Carlo, we are interested in the potential at a point $\boldsymbol{r}$ due to a point charge at $\boldsymbol{r}'$, given everything else in the problem. This is embodied in the idea of the Green's function, defined as

$$\begin{aligned} \nabla'^2 \ G(\boldsymbol{r},\boldsymbol{r}') &= -\delta(\boldsymbol{r}-\boldsymbol{r}')\boldsymbol{r},\boldsymbol{r}' \in \Omega \\ G(\boldsymbol{r},\boldsymbol{r}') &= 0, \quad \boldsymbol{r}' \in \partial\Omega \end{aligned} \tag{3}$$

where Ω is *any* volume within the region, and $\partial\Omega$ is the surface of that volume. Without loss of generality let's denote by Ω the entire system volume. The second equation is a consequence of the Dirichlet boundary condition. In terms of this Green's function, the potential $\Phi(\boldsymbol{r})$ at any point $\boldsymbol{r}$ is given by[26]

$$\Phi(\boldsymbol{r}) = \int_\Omega \rho(\boldsymbol{r}')G(\boldsymbol{r},\boldsymbol{r}')d^3\boldsymbol{r}' + \int_{\partial\Omega} d^2\boldsymbol{r}' \cdot \boldsymbol{\nabla} G(\boldsymbol{r},\boldsymbol{r}')\Phi(\boldsymbol{r}') \tag{4}$$

i.e. the potential has contributions both from the volume charges (like doped charges) and the boundary potential (like voltages applied at metal gates on the surface). Also, we need to know the potential $\Phi(\boldsymbol{r}')$ on the surface. Thus the Green's function plays a crucial role in the interparticle interactions, if we know it then we have solved the problem. We stress again that Eq.(4) holds for any volume Ω.

As we will show, a method called the domain Green's function Monte Carlo (dGFMC)[27], originally developed to solve Schrödinger's equation evaluates both integrals in Eq.(4) simultaneously. This is not surprising given the connection between diffusion (like imaginary time Schrödinger's equation), Brownian motion and potential theory. The key idea is to realize that we can write Eq.(4) for any domain $\mathcal{D}$ of any arbitrary shape instead of Ω which is the entire system. This will require a redefinition of the Green's function $G_\mathcal{D}(\boldsymbol{r},\boldsymbol{r}')$ to be defined only within the domain $\mathcal{D}$ with surface $\partial\mathcal{D}$. Thus,

$$\begin{aligned} \nabla'^2 G_\mathcal{D}(\boldsymbol{r},\boldsymbol{r}') &= -\delta(\boldsymbol{r}-\boldsymbol{r}'), \quad \boldsymbol{r},\boldsymbol{r}' \in \mathcal{D} \\ G_\mathcal{D}(\boldsymbol{r},\boldsymbol{r}') &= 0 \text{ if } \boldsymbol{r}' \in \partial\mathcal{D} \text{ or outside } \mathcal{D}. \end{aligned} \tag{5}$$

Since the choice of the domain $\mathcal{D}$ is arbitrary, we should choose it such that $G_\mathcal{D}(\boldsymbol{r},\boldsymbol{r}')$ has a known analytic form and is inexpensive to compute. In terms of this domain Green's function, the potential in Eq.(4) becomes

$$\Phi(\boldsymbol{r}) = \int_\mathcal{D} \rho(\boldsymbol{r}')G_\mathcal{D}(\boldsymbol{r},\boldsymbol{r}')d^2\boldsymbol{r}' + \int_{\partial\mathcal{D}} d^2\boldsymbol{r}' \cdot \nabla G_\mathcal{D}(\boldsymbol{r},\boldsymbol{r}')\Phi(\boldsymbol{r}') \tag{6}$$

The first integral is known exactly, and the second integral is very similar to that in Eq.(1); in fact if the gradient term is constant, then they are identical up to a constant factor. Hence the same WOS algorithm can evaluate this term, provided we generalize it to the arbitrary domain $\mathcal{D}$ and sample its surface $\partial\mathcal{D}$, not uniformly as in WOS, but according to $\nabla G_\mathcal{D}(\boldsymbol{r},\boldsymbol{r}')$. We have thus generalized WOS to a "walk on domains" $\mathcal{D}_0, \mathcal{D}_1 \ldots$ instead of spheres. The iterative nature of Eq.(6) is inherent to the WOS algorithm. Accumulating contributions of $G_\mathcal{D}(\boldsymbol{r}_k,\boldsymbol{r}_{k+1})$ from each domain $\mathcal{D}_k$ along the walk and averaging over several such walks will provide an estimate of $\Phi(\boldsymbol{r})$. To evaluate the first integral of Eq.(6) we sample a point $\boldsymbol{s}$ in the domain according to $G_\mathcal{D}(\boldsymbol{r},\boldsymbol{r}')$ and accumulate $\rho(\boldsymbol{s})$ (with proper normalization)[28]. Thus the "Walk On Spheres/Domains" is a general algorithm to solve the potential problem. For completeness we should

also mention that the Green's function for the entire system defined over Ω is given by

$$G(\boldsymbol{r}, \boldsymbol{r}') = G_{\mathcal{D}}(\boldsymbol{r}, \boldsymbol{r}') + \int_{\partial \mathcal{D}} d^2 \boldsymbol{r}'' \cdot \boldsymbol{\nabla} G_{\mathcal{D}}(\boldsymbol{r}, \boldsymbol{r}'') G(\boldsymbol{r}'', \boldsymbol{r}')$$
(7)

and our walk is implicitly constructing this Green's function.

Though theoretically the domain shape can be arbitrary, in practice it is wise to choose a shape for which $G_{\mathcal{D}}(\boldsymbol{r}, \boldsymbol{r}')$ is known and inexpensive to compute. If we restrict ourselves to spherical domains, the Green's function has a particularly simple form. For a sphere of radius d centered at $\boldsymbol{r}$,

$$G_{\mathcal{D}}(\boldsymbol{r}, \boldsymbol{r}') = \frac{1}{4\pi\varepsilon}\left(\frac{1}{|\boldsymbol{r} - \boldsymbol{r}'|} - \frac{1}{d} \right),$$
(8)

and $d^2 \boldsymbol{r}' \cdot \nabla G_{\mathcal{D}}(\boldsymbol{r}, \boldsymbol{r}') = d^2 r$, i.e. the domain surface should be sampled uniformly, exactly as in WOS. Also we see that this captures the $1/r$ Coulomb term but also provides the corrections due to the boundary conditions.

This algorithm also naturally accounts for the quantum Monte Carlo walker density which is simply $\sum_j Q_j \delta(\boldsymbol{r} - \boldsymbol{q}_j)$, where Q_j is the charge of j-th particle at $\boldsymbol{q}_j$. The volume integral $\int \rho G d^3 r$ of Eq.(4) merely becomes $\sum_j Q_j G(\boldsymbol{r}, \boldsymbol{q}_j)$, which we have already described how to compute. To use this algorithm with quantum Monte Carlo we simply need to convert the potential $\Phi(\boldsymbol{R}_m)$ into the potential energy $V(\boldsymbol{R}_m)$.

The total potential energy of the configuration is

$$V(\boldsymbol{R}_m) = \sum_{i=1}^{N} Q_i \left[\Phi_{\text{Gate}}(\boldsymbol{q}_i) + \frac{1}{2} \sum_{j \neq i} Q_j G(\boldsymbol{q}_i, \boldsymbol{q}_j) \right] + \sum_{i=1}^{N} V_{\text{self}}(\boldsymbol{q}_i), \qquad \{\boldsymbol{q}_i\} \in \boldsymbol{R}_m.$$
(9)

$V_{\text{self}}(\boldsymbol{q}_i)$ is the effect of the charges induced in the environment by the particle at $\boldsymbol{q}_i$ itself. This effect manifests itself in the Green's function for the particle $G(\boldsymbol{q}_i, \boldsymbol{q}_i)$ which is of course divergent due to the inherent Coulomb divergence of any charged particle. So,

$$V_{\text{self}}(\boldsymbol{q}_i) = \frac{Q_i^2}{2} \lim_{\boldsymbol{r} \to \boldsymbol{q}_i} \left[G(\boldsymbol{r}, \boldsymbol{q}_i) - \frac{1}{4\pi\varepsilon} \frac{1}{|\boldsymbol{r} - \boldsymbol{q}_i|} \right].$$

For the spherical domain, this simplifies beautifully; the $1/r$ divergence in Eq.(8) cancels with that in the self term above leaving a contribution of $-Q_i^2/(2d_0)$ from the first domain. The remainder is an extra contribution from each subsequent domain of the same WOS; together, this accounts for the entire potential energy.

IV. IMPROVING EFFICIENCY

Convergence properties of the WOS algorithm have been extensively studied by Muller[21] and de Laurentis[28].

For an N-particle system, each walk takes on average $n = \mathcal{O}(|\log \delta|)$ (see Fig.(1)) steps to converge. A separate walk has to be started from each particle at $\boldsymbol{q}_i$ $\forall i$ in the sum of Eq.(9). An N-fold efficiency can be gained if the same walk can estimate the potential at points neighboring the origin of the walk. If the walkers $\{\boldsymbol{R}\}$ are all confined within a small region, then an algorithm by Pickles[29] to calculate electric fields, can be adapted for this purpose.

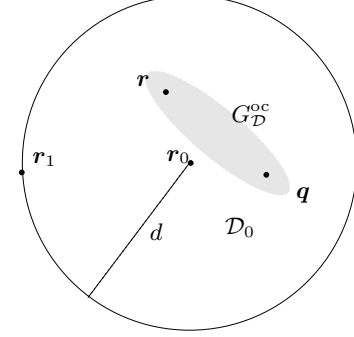FIG. 2: Sampling the interaction between points $\boldsymbol{q}$ and $\boldsymbol{r}$ inside the domain $\mathcal{D}_0$ centered at $vecr_0$.

The basic ideas and equations have already been introduced. In the previous section we generalized the Mean Value Theorem Eq.(1) (for spherical domains), to domains of arbitrary shapes by means of

$$\Phi(\boldsymbol{q}) = \int_{\partial \mathcal{D}} d^3 \boldsymbol{r}' \cdot \boldsymbol{\nabla} G_{\mathcal{D}}(\boldsymbol{q}, \boldsymbol{r}') \Phi(\boldsymbol{r}').$$

For the sphere centered on the point $\boldsymbol{q}$ with $G_{\mathcal{D}}$ given by Eq.(8), this reduces to Eq.(1) which is uniform sampling over the domain surface. However, we could as well use an "off-centered" Green's function which would account for the potential not just at the domain center but at neighboring points as well. So for a sphere of radius d and centered at $\boldsymbol{r}_0$, we need $G_{\mathcal{D}}(\boldsymbol{q}, \boldsymbol{r})$ between any two points $\boldsymbol{q}$ and $\boldsymbol{r}$ inside the sphere. This is easily obtained from the method of images[30]

$$G_{\mathcal{D}}^{\text{oc}}(\boldsymbol{q}, \boldsymbol{r}) = \frac{1}{4\pi\varepsilon} \left[\frac{1}{|\boldsymbol{q} - \boldsymbol{r}|} - \frac{d}{|\boldsymbol{r} - \boldsymbol{r}_0||\boldsymbol{q} - (d/r)^2 \boldsymbol{r}|} \right].$$

Sampling the point $\boldsymbol{r}_1$ on the domain surface (see Fig.(2)) could still be uniform if the walk is weighted by a factor of $w_i = \nabla G_{\mathcal{D}}^{\text{oc}}(\boldsymbol{q}_i, \boldsymbol{r}_1) = d(d^2 - q_i^2)/|\boldsymbol{q}_i - \boldsymbol{r}_1|^3$ for each particle at $\boldsymbol{q}_i$.

So the modification needed to WOS is very simple. The first sphere is centered at some common point, say the centroid of the walker configuration. The point $\boldsymbol{r}_1$ is sampled uniformly on the domain surface, and the weight $w_i \equiv w(\boldsymbol{q}_i, \boldsymbol{r}_1)$ is computed for each particle. From then on, the walk continues using centered spheres using Eq.(8). The potential $\Phi(\boldsymbol{q}_i)$ sampled from this walk is obtained by weighting the walk by the prerecorded

$w(\boldsymbol{q}_i, \boldsymbol{r}_1)$s. Thus the contribution of the applied potential, i.e. the $Q_i\Phi(\boldsymbol{q}_i)$ part of Eq.(9) becomes

$$\frac{1}{\mathcal{N}}\sum_{n=1}^{\mathcal{N}} Q_i w(\boldsymbol{q}_i, \boldsymbol{r}_1^{(n)})\Phi_{\mathrm{app}}(\boldsymbol{r}_n^\star).$$

However, if the particle position $\boldsymbol{q}_i$ happens to be far from the domain center $\boldsymbol{r}_0$, i.e. near the surface of the first domain, then the estimate of $\Phi(\boldsymbol{q}_i)$ is dominated by only a few walks with large weights and the noise in the estimate is magnified. A good rule of thumb is to choose the first sphere of radius d_0 such that $|\boldsymbol{q}_i - \boldsymbol{r}_0| \le d_0/2, \forall i$.

This method can be directly used for a fast and efficient estimation. Suppose we perform an initial calculation to generate $\mathcal{N}$ runs, where the n-th run samples the point $\boldsymbol{r}_1^{(n)}$ on the surface of the first domain, and the run ends on the device boundary at a point $\boldsymbol{r}_n^\star$. If we tabulate this information $\{\boldsymbol{r}_1^{(n)}, \Phi_{\mathrm{app}}(\boldsymbol{r}_n^\star)\} \forall n = 1,\ldots,\mathcal{N}$, then at any later time we can obtain a quick estimate of the potential at any point $\boldsymbol{q}_i$ by simply evaluating

$$\tilde{\Phi}(\boldsymbol{q}_i) = \frac{1}{\mathcal{N}'}\sum_{n}^{\mathcal{N}'} w(\boldsymbol{q}_i, \boldsymbol{r}_1^n)\Phi_{\mathrm{app}}(\boldsymbol{r}_n^\star), \quad (\mathcal{N}' \le \mathcal{N})$$

without the need for any more time consuming walks. The accuracy will of course depend on $\mathcal{N}'$. Generating all our estimates from the same finite set of data can lead to undesired correlations, which can be reduced by simply limiting the number of estimates according to the size of the data used. A good rule of thumb is to obtain no more than $\mathcal{N}$ separate estimates (for e.g. $\tilde{\Phi}(\boldsymbol{q}_i), i = 1,\ldots,\mathcal{N}$) from a data set of size $\mathcal{N}$.

Many further improvements are possible. As will be shown below, this approach (of using off-centered domains) can be slightly modified to be used as one of many variance reduction techniques which can be easily incorporated within the WOS scheme. However effectiveness of each technique will depend on the system or rather on the various competing contributions to the potential. Here we present a general overview of some of these strategies. In section VI, we will discuss these approaches in light of a simple application. The contributions to the potential come mainly from the effect of the applied boundary voltages and interaction between the volume charges. The choice of approach to reduce noise will depend on which of these contributions dominate.

Consider for example, the approach described above of obtaining the potential at points neighboring the walk-origin. This can be used to reduce the variance in the contribution of the applied boundary potentials. Suppose we know the potential $\Phi(\boldsymbol{r}_c)$ at some point $\boldsymbol{r}_c$ in the first domain (it could be the origin of the walk). A stochastic estimate of the quantity $\Delta\Phi_{ic} = \langle \tilde{\Phi}(\boldsymbol{q}_i) - \tilde{\Phi}(\boldsymbol{r}_c)\rangle$ using the weight $w_{ic} = w(\boldsymbol{q}_i) - w(\boldsymbol{r}_c)$ will have a much smaller variance than subtracting the separate estimates. This is simply a form of correlated sampling. Then we can easily obtain $\Phi(\boldsymbol{q}_i) = \Phi(\boldsymbol{r}_c) + \Delta\Phi_{ic}$.

Importance sampling is another technique that can be considered when we have some a priori knowledge of the potential profile; we can preferentially sample the *important* regions of the device and this will reduce variance. The form of the importance function will depend on the device geometry and we will discuss a specific example in section VI. For now, we will simply demonstrate a zero variance principle, i.e. if we know the potential exactly, then the potential itself is the optimal importance function and WOS can recover the potential without any noise in the estimate. This by itself is an uninteresting result but the what is important to note (and will be demonstrated later) that the variance can be reduced arbitrarily if even an approximate importance function can be arbitrarily improved to approach the optimal form.

The WOS integral is of the form

$$\Phi(\boldsymbol{r}) = \int \nabla G_{\mathcal{D}}(\boldsymbol{r}, \boldsymbol{r}')\Phi(\boldsymbol{r}')d^2\boldsymbol{r}'$$

For the spherical domain, a choice of importance function $I(\boldsymbol{r})$ leads to

$$\Phi(\boldsymbol{r}) = \int \frac{\Phi(\boldsymbol{r}')}{\mathbb{N}I(\boldsymbol{r}')/I(\boldsymbol{r})}\left[\mathbb{N}\frac{I(\boldsymbol{r}')}{I(\boldsymbol{r})}\frac{\sin\theta d\theta}{2}\frac{d\phi}{2\pi}\right],$$

we sample according to the term within the square brackets, and carry a weight $I(\boldsymbol{r})/\mathbb{N}I(\boldsymbol{r}')$ for each domain. Here $\mathbb{N}$ is the normalization, and $\boldsymbol{r}$ is the center of the domain while $\boldsymbol{r}'$ is the next point in the walk sampled on the surface of that domain. As the walk proceeds $\boldsymbol{r}_0 \to \boldsymbol{r}_1 \ldots \boldsymbol{r}_m$, the accumulated weight becomes

$$\frac{1}{\mathbb{N}^{m-1}}\frac{I(\boldsymbol{r}_0)}{I(\boldsymbol{r}_1)}\frac{I(\boldsymbol{r}_1)}{I(\boldsymbol{r}_2)}\cdots\frac{I(\boldsymbol{r}_k)}{I(\boldsymbol{r}_{k+1})}\cdots\frac{I(\boldsymbol{r}_{m-1})}{I(\boldsymbol{r}_m)} = \frac{1}{\mathbb{N}^{m-1}}\frac{I(\boldsymbol{r}_0)}{I(\boldsymbol{r}_m)},$$

the walk reaches the boundary at $\boldsymbol{r}_m$ and picks up the potential $\Phi(\boldsymbol{r}_m)$, the accumulated term from the walk is $I(\boldsymbol{r}_0)\Phi(\boldsymbol{r}_m)/\mathbb{N}^{m-1}I(\boldsymbol{r}_m)$. If the importance function is chosen such that $I(\boldsymbol{r}) = \Phi(\boldsymbol{r})$, then it is seen from the Mean Value Theorem above that the importance function is normalized i.e. $\mathbb{N} = 1$, and the accumulated contribution from *each* walker is $\Phi(\boldsymbol{r}_0)$ leading to zero variance. If the importance function is not optimal, then the normalization needs to be carried along and the zero variance principle doesn't hold any more.

Other standard variance reduction techniques may also be considered. Antithetic variates can be easily implemented by constructing pairs of walks; the walks in each pair will sample opposite points on the surface of the first domain. However, the drawback of the method is that this can be constructed only for the first domain, beyond this the walks will proceed independently. We find this to yield only a marginal improvement even when the potential profile is antisymmetric about the origin of the walk. In general this method will not be very effective for arbitrary potential profiles.

V. QMC WITH A STOCHASTICALLY SAMPLED POTENTIAL

Now we demonstrate how quantum Monte Carlo methods can incorporate the stochastically sampled potential. In this regard we will study the two most popular methods, namely variational and diffusion Monte Carlo. Note that we have two different samplings or "walks", one to solve the Schrödinger's equation which we will refer to by the standard name "walkers" described before, and the walks needed to solve the classical potential problem, which we'll refer to as "runs" or "runners" to distinguish them from the walkers.

A. Variational Monte Carlo

The variational approach posits a functional form of the trial wave-function $\Psi_T(\boldsymbol{\alpha})$ which depends on a set of parameters $\{\boldsymbol{\alpha}\}$[2,3]. Minimization of the energy, (or variance or a mixture of both) with respect to the set $\{\boldsymbol{\alpha}\}$, by methods like correlated sampling[31,32] gives the variational estimate of the energy.

$$\min_{\{\boldsymbol{\alpha}\}}\langle\Psi_T(\boldsymbol{\alpha})|\mathcal{H}|\Psi_T(\boldsymbol{\alpha})\rangle = E_{\text{VMC}},$$

where $\mathcal{H} = -\frac{1}{2}\nabla^2 + V$ is the Hamiltonian in a.u. The minimization aside, $E = \langle\Psi_T|\mathcal{H}|\Psi_T\rangle$ (dependence on $\boldsymbol{\alpha}$ dropped for convenience) is simply a multi-dimensional integral which is performed by the Monte Carlo . The estimator for this integral is called the local energy

$$E_L(\boldsymbol{R}) = \frac{\mathcal{H}\Psi_T(\boldsymbol{R})}{\Psi_T(\boldsymbol{R})} = -\frac{1}{2}\frac{\nabla^2\Psi_T(\boldsymbol{R})}{\Psi_T(\boldsymbol{R})} + V(\boldsymbol{R}). \quad (10)$$

A set of randomly distributed configurations $\{\boldsymbol{R}\}$ called walkers, are sampled according to the Metropolis algorithm[33,34] to generate the distribution Ψ_T^2, i.e. $\mathbb{P}(\boldsymbol{R}_m) = \Psi_T^2$, where $\mathbb{P}$ is the probability distribution function (unnormalized). It is important to note here that this sampling *does not* involve a knowledge of the potential profile $V(\boldsymbol{r},\boldsymbol{R}_m)$ for the walker $\boldsymbol{R}_m$. If M configurations are generated, then (after equilibration)

$$\langle V\rangle_{\text{VMC}} = \int V(\boldsymbol{R})\Psi_T^2(\boldsymbol{R})d^{3N}\boldsymbol{R} \approx \frac{1}{M}\sum_{m=1}^{M} V(\boldsymbol{R}_m),$$
$$(11)$$

is an estimate of the potential energy of the state Ψ_T. Here $V(\boldsymbol{R}_m)$ is the exact potential energy of the walker $\boldsymbol{R}_m$ distributed according to Ψ_T^2. However even if we use a potential $\tilde{V}(\boldsymbol{R}_m)$ which is stochastic,

$$\langle V(\boldsymbol{R}_m)\rangle_{\text{VMC}} = \langle\tilde{V}(\boldsymbol{R}_m)\rangle_{\text{WOS}} \quad (12)$$

This is seen from the following. The stochastic potential can be expressed as $\tilde{V}(\boldsymbol{R}_m) = V(\boldsymbol{R}_m) + \Delta(\boldsymbol{R}_m)$,

where in the limit of large samples, the error $\Delta(\boldsymbol{R}_m)$ is normally distributed with mean zero. Hence $\langle\Delta(\boldsymbol{R}_m)\rangle$ is,

$$\lim_{M\to\infty}\frac{1}{M}\sum_{m=1}^{M}\Delta(\boldsymbol{R}_m) = \int d\boldsymbol{r}\mathbb{P}(\boldsymbol{R}_m)\left[\int\Delta\mathbb{P}(\Delta)d\Delta\right] = 0,$$
$$(13)$$

simply from the zero mean property of the error Δ. Thus the variational Monte Carlo algorithm can simply use the stochastic potential $\tilde{V}(\boldsymbol{R}_m)$ without any other modifications. The primary requirement for variational Monte Carlo to work is that the distribution $\mathbb{P}(\Delta)$ have zero mean.

Consider a simple system with a known potential profile $V(\boldsymbol{r})$. Suppose to calculate the expectation of the potential energy corresponding to some given state Ψ_T (using variational Monte Carlo) with a target error of δV, we need N_w walkers. We can perform the same calculation using the stochastic potential instead of the known form, and using N_r runners (as described at the beginning of this section) for each walker, a total of $N_w N_r$ samples. Numerical experiments show that the the the calculation is optimal when $N_r = 1$ and N_w is chosen such that an independent stochastic calculation of the potential $\Phi(\boldsymbol{P})$ at some point $\boldsymbol{P}$ using N_w runners yield an error $\delta\Phi \sim \mathcal{O}(\delta V)$. This is because variational Monte Carlo is insensitive to the accuracy of the potential sampled, as long as there are enough samples. So it is optimal to sample $\tilde{V}(\boldsymbol{R})$ for more configurations using more walkers, than increasing the accuracy of each estimate.

Optimization of the trial wave-function Ψ_T can easily be carried out by correlated sampling as usual, except that WOS can optimize only the variational energy and not the variance of the energy. One important distinction from usual computer algorithms needs to be emphasized. During the initial variational Monte Carlo run to generate the configurations, programs record the walker configurations, but usually not the corresponding local potential energies $V(\boldsymbol{R}_m)$ (the potential part of the local energy which depends on the wave-function only through the walker distribution). When the optimizer modifies the parameters $\boldsymbol{\alpha}$, changing the trial wave-function $\Psi_T(\boldsymbol{\alpha})$, the corresponding local Kinetic energy $-\frac{1}{2}\nabla^2\Psi_T/\Psi_T$ also changes. And the local energy of the walker is calculated anew because this saves storage and a known analytic potential is usually not too expensive to recompute.

However, recomputing the stochastic potential would in general produce a different estimate than before, i.e. $\tilde{V}(\boldsymbol{R}_m)$ will be different each time we recompute it. This will introduce an error which will not cancel on averaging, and hence destroy the optimization. This is easily remedied by simply recording the estimate of the local potential energy $\tilde{V}(\boldsymbol{R}_m)$ while recording the configurations $\{\boldsymbol{R}\}$. This will eliminate the overhead of recomputing the potential which can be expensive, the cost being a marginal increase in storage. Using the same local potential for a given configuration at every iteration of the optimization process we ensure that we minimize

the correct estimate of the local energy.

B. Diffusion Monte Carlo

The stochastic potential approach is particularly compatible with variational Monte Carlo because VMC is linear in energy, and thus able to take advantage of Eq.(12). Exact Green's function Monte Carlo methods are also linear in energy and would be able to take advantage of this approach. However, diffusion Monte Carlo is not an exact Green's function method because of the short time approximation which simulates the Green's function by diffusion and branching. This makes the use of WOS with diffusion Monte Carlo not as straightforward as with variational Monte Carlo.

To see why this is the case, we review the basic ideas of the diffusion Monte Carlo algorithm very briefly. For practical details regarding implementation, see reviews or books like[2,3,35]. The Schrödinger's equation in imaginary time

$$-\partial_t \psi(\mathbf{R}, t) = (\mathcal{H} - E_T)\psi(\mathbf{R}, t)$$

can be transformed into an integral equation of the form

$$f(\mathbf{R}, t + \tau) = \int G(\mathbf{R}, \mathbf{R}'; \tau)f(\mathbf{R}', t)d\mathbf{R}', \qquad (14)$$

where $f(\mathbf{R}, t) = \psi(\mathbf{R}, t)\Psi_T(\mathbf{R}, t)$ is a product of a known "trial" or "guiding" function Ψ_T and the eigenfunction ψ. E_T is an energy offset and $G(\mathbf{R}, \mathbf{R}'; \tau)$ is the Green's function or propagator. The integral equation is solved iteratively by starting with an initial distribution $f_{\text{init}} = \psi_{\text{init}}\Psi_T$ or rather a set of walkers distributed according to f_{init}. Repeated application of the Green's function to this state projects out the lowest energy state not orthogonal to ψ_{init}.

The essence of the algorithm is in calculation of this Green's function $G(\mathbf{R}, \mathbf{R}'; \tau)$. If E_L and E_L' are the local energies at points $\mathbf{R}$ and $\mathbf{R}'$ respectively, then within diffusion Monte Carlo the Green's function is approximated by

$$G(\mathbf{R}, \mathbf{R}'; \tau) \approx G_{\text{diff}}(\mathbf{R}, \mathbf{R}'; \tau)G_B(E_L, E_L'; \tau), \qquad (15)$$

where

$$G_{\text{diff}}(\mathbf{R}, \mathbf{R}'; \tau) = \frac{1}{(2\pi\tau)^{3N/2}} \exp\left[-\frac{(\mathbf{R} - \mathbf{R}' - \tau\mathbf{v}(\mathbf{R}'))^2}{2\tau}\right],$$

and

$$G_B(E_L, E_L'; \tau) = \exp[-(E_L(\mathbf{R}) + E_L(\mathbf{R}') - 2E_T)\tau/2]. \qquad (16)$$

G_{diff} is the Green's function for a diffusion process, $\mathbf{v} = \nabla \ln|\Psi_T(\mathbf{R})|$ is a drift velocity, N is the number of particles and G_B is a weight factor. This approximation holds for small time step τ.

For improved stability and convergence most algorithms implement the weight factor G_B by a "branching" or "birth/death" process in which $n_B = \text{int}[G_B + \xi]$ copies of the walker survive to the next step[36]. Here ξ is a random number drawn uniformly in the range $(0, 1]$. Thus in the regions of high potential energy G_B is small and the walkers disappear, while in the regions of low potential energy G_B is large and the walkers proliferate. This is a marked difference from the variational Monte Carlo algorithm since here the number of walkers and hence the walk itself depends on our estimate of the potential.

We note in passing that the local energy as defined in Eq.(10) is the sum of kinetic and potential terms. But all that is germane to the following discussion is contained in the simplest unsymmetrized form of the weight G_B. Thus

$$\mathbb{G}_B(V, \tau) = \exp\left[-V\tau\right]$$

which depends only on the potential energy $V(\mathbf{R})$, is enough to illustrate all the issues of using a stochastic potential with diffusion Monte Carlo. $\mathbb{G}_B(E_L)$ is simply $\mathbb{G}_B(V)$ with a factor which is independent of the potential and hence not relevant to the ensuing discussion. These considerations greatly simplify the notation in the present discussion. However in the numerical experiments in section VI we use the importance sampled diffusion Monte Carlo with the Green's function given by Eqs.(15) and (16).

Sampling with a stochastic potential has serious implications for the branching. Unlike the situation in variational Monte Carlo the effect here is nonlinear (exponential) and hence a simple averaging will not get rid of the noise in the potential.. If we branch using a stochastically obtained potential $\tilde{V}$, then in effect we will be branching on average according to $\langle \exp[-\tilde{V}\tau] \rangle$. This is however not equal to $\exp[-\langle\tilde{V}\rangle\tau]$ (i.e. $\exp[-\langle V\rangle\tau]$ since $\langle\tilde{V}\rangle = V$) which is the branching we need. But nevertheless,

$$\langle \exp[-\tilde{V}\tau] \rangle = \exp[-\langle V \rangle \tau] + \mathcal{O}(\tau^2), \qquad (17)$$

i.e. the branching obtained by using the stochastic potential is correct to second order in τ. Hence this poses a limitation on the size of the time step that we can use. However, the most important factor in the error is the prefactor of τ^2 which depends on the device geometry in the problem. This error is unacceptable since our main motivation of sampling the potential stochastically is to improve the accuracy over other alternative methods. To improve the accuracy of the branching we could use a large enough number of runners to estimate the potential so that the noise is negligible, but this is *very* expensive and contrary to the philosophy of improving accuracy using a stochastic estimate of the potential.

To overcome this problem we use the penalty method[37] which modifies a random walk to accept noisy energies. The major part of the following discussion is a direct application of the penalty method. However as we will

show there are also some very subtle and special considerations in the present use of the penalty method. Let $\tilde{V}$ be a WOS potential estimate for some configuration $\boldsymbol{R}$, while V is the exact potential for the same configuration. $\mathbb{G}_B(V)$ is the previously defined branching term using the exact potentials, while $\tilde{\mathbb{G}}_B(\tilde{V})$ is the same expression using the WOS potentials. This branching factor will definitely be biased, and hence we introduce a modified branching factor $g_B(\tilde{V})$ which depends only on the estimate $\tilde{V}$. Let $\mathbb{P}(\tilde{V})$ be the probability for obtaining the estimate $\tilde{V}$. For the calculation using the WOS potential to be accurate, we require that the average branching must satisfy

$$\langle g_B \rangle \equiv \int_{-\infty}^{\infty} d\tilde{V} \, \mathbb{P}(\tilde{V}) g_B(\tilde{V}) = \mathbb{G}_B(V, \tau), \qquad (18)$$

so that even with a stochastic potential the walker would branch correctly on average.

In order to make progress we have to assume a form for the probability distribution $\mathbb{P}(\tilde{V})$. In the limit of large number of runners, the central limit theorem guarantees that the distribution will be normal, but our primary goal is to use as few runners as possible and hence the distribution will certainly be somewhat different from a standard normal. Nevertheless, for now we assume a normal distribution with mean V and a known variance σ^2.

$$\mathbb{P}(\tilde{V}) = \frac{1}{\sqrt{2\pi\sigma^2}} \exp\left[-\frac{1}{2}\frac{(\tilde{V}-V)^2}{\sigma^2}\right]. \qquad (19)$$

The variance σ^2 is not known in general but we assume that we know it for now; the penalty method estimates the necessary corrections which we will briefly mention at the end of this section.

A simple solution for the modified branching term $g_B(\tilde{V})$ which satisfies the above considerations is

$$g_B(\tilde{V}) = \exp[-(\tilde{V} + \sigma^2\tau/2)\tau]. \qquad (20)$$

To see that this indeed satisfies the condition that $\langle g_B(\tilde{V})\rangle = \mathbb{G}_B(V)$, consider a simple form for the modified branching $g_B = \gamma(\sigma^2)\tilde{\mathbb{G}}_B(\tilde{V})$ along with the probability distribution Eq.(20) and substitution in Eq.(18) leads directly to the form of $\gamma(\sigma^2) = \exp[-\sigma^2\tau^2/2]$. Since σ^2 is always positive, this shows that we rely less on a noisy potential and branch less than what we would if the estimate was exact.

This can be easily extended to the importance sampled branching factor

$$g_B(\boldsymbol{R}, \boldsymbol{R}') = \exp\left[-(\tilde{E}_L + \tilde{E}_L' + (\sigma^2 + \sigma'^2)\frac{\tau}{2} - 2E_T)\frac{\tau}{2}\right] \qquad (21)$$

where $\tilde{E}_L(\tilde{V})$ is the local energy using the stochastic estimate of the potential. The analysis up to this point is a direct extension of the penalty method of Ceperley and Dewing[37], but certain special considerations need to be made to apply the penalty method in the present context.

Branching according to the above factor in Eq.(21) instead of the branching of Eq.(16) will produce the correct expectation of observables independent of the WOS potential $\tilde{V}$, for example the kinetic energy. If however the observable is dependent on the stochastic potential $\tilde{V}$, like the potential energy itself, we have to take care of the correlations between the observable and the branching factor. This can be seen from considering the expectation of the energy which is usually evaluated from the mixed estimator[2] given by

$$E_{\text{DMC}} = \frac{\langle\psi_0|\mathcal{H}|\Psi_T\rangle}{\langle\psi_0|\Psi_T\rangle} = \lim_{\tau\to\infty}\frac{\int d\boldsymbol{R} f(\boldsymbol{R}, \tau)E_L(\boldsymbol{R})}{\int d\boldsymbol{R} f(\boldsymbol{R}, \tau)} = \lim_{\tau\to\infty}\frac{\int d\boldsymbol{R} d\boldsymbol{R}' G(\boldsymbol{R}, \boldsymbol{R}'; \tau)f_{\text{init}}(\boldsymbol{R}')E_L(\boldsymbol{R})}{\int d\boldsymbol{R} d\boldsymbol{R}' G(\boldsymbol{R}, \boldsymbol{R}'; \tau)f_{\text{init}}(\boldsymbol{R}')} = \frac{1}{M}\sum_m E_L(\boldsymbol{R}_m) \qquad (22)$$

where we have simply used the form of Eq.(14) starting with the initial distribution f_{init}. If however, we use diffusion Monte Carlo with a stochastic potential, then the expectation of the local energies become

$$\tilde{E}_{\text{DMC}} = \frac{1}{M}\sum_m \tilde{E}_L(\tilde{V}, \boldsymbol{R}_m) = \frac{\int d\boldsymbol{R} d\boldsymbol{R}' d\tilde{V} d\tilde{V}' d\tilde{V}'' \tilde{g}(\boldsymbol{R}, \boldsymbol{R}', \tilde{V}, \tilde{V}'; \tau)f_{\text{init}}(\boldsymbol{R}')\mathbb{P}(\tilde{V})\mathbb{P}(\tilde{V}, \tilde{V}'')\tilde{\mathbb{E}}_L(\tilde{V}'', \boldsymbol{R})}{\int d\boldsymbol{R} d\boldsymbol{R}' d\tilde{V} d\tilde{V}' \tilde{g}(\boldsymbol{R}, \boldsymbol{R}', \tilde{V}, \tilde{V}'; \tau)f_{\text{init}}(\boldsymbol{R}')\mathbb{P}(\tilde{V})\mathbb{P}(\tilde{V}')}. \qquad (23)$$

Here $\tilde{g}(\boldsymbol{R}, \boldsymbol{R}', \tilde{V}, \tilde{V}'; \tau) \approx G_{\text{diff}}(\boldsymbol{R}, \boldsymbol{R}'; \tau)\tilde{g}_B(\tilde{V}, \tilde{V}'; \tau)$ is the modified Green's function, $\mathbb{P}(\tilde{V})$ is the distribution of the WOS estimate, and $\mathbb{P}(\tilde{V}, \tilde{V}'')$ is the joint probability distribution of obtaining the estimates $\tilde{V}$ and $\tilde{V}''$. $\tilde{V}''$ is the estimate used to evaluate the "modified" local energy $\tilde{\mathbb{E}}_L(\tilde{V}'', \boldsymbol{R})$. The estimate $\tilde{E}_{\text{DMC}}$ given by Eq.(23) is not in general equal to the desired estimate E_{DMC}. The

problem and a solution can be seen from a simple analysis and a modification of the estimator that will give the desired result. The simplest way to accomplish this is to require the numerators and denominators in Eq.(22) and Eq.(23) to be equal separately. Our previous choice of $\tilde{g}_B$ makes the denominators equal. This is seen from the

fact that

$$\tilde{g} = \gamma G_{\text{diff}} \tilde{G}_B = [\gamma(\sigma^2, \sigma'^2)e^{-\Delta\tau}e^{-\Delta'\tau}]G(\boldsymbol{R}, \boldsymbol{R}')$$

where as in prior notation $\Delta = \tilde{V} - V$ and similarly for Δ'. Substitution into the integral in the denominator of Eq.(23) proves the result.

The numerator is more tricky, and depends on the algorithm for obtaining the estimator. The part of the estimator that does not depend on the WOS estimate, i.e. the kinetic energy is does not pose any trouble, it integrates in the same way as the denominator. The potential part could be obtained in two different ways. In the simplest case, we could use separate and independent estimates $\tilde{V}$ and $\tilde{V}''$ for the branching and the estimator. In this case the probabilities would be uncorrelated and $\mathbb{P}(\tilde{V}, \tilde{V}'') = \mathbb{P}(\tilde{V})\mathbb{P}(\tilde{V}'')$. In this case, the integrals again become similar to those explained before and no modification is necessary, i.e. $\tilde{\mathbb{E}}_L = \tilde{E}_L$. We will call this the uncorrelated penalty correction. If however, we use the same potential $\tilde{V}$ for both the branching and the estimator, then the two estimates are identical, i.e. $\mathbb{P}(\tilde{V}, \tilde{V}'') = \delta(\tilde{V} - \tilde{V}'')\mathbb{P}(\tilde{V})$. In this case a modification of the form $\tilde{\mathbb{E}}_L(\boldsymbol{R}) = \tilde{E}_L(\tilde{V}, \boldsymbol{R}) + \sigma^2\tau$ makes the estimator $\tilde{E}_{\text{DMC}}$ equal to the desired $\tilde{E}_{\text{DMC}}$. This can be seen from simply substituting and performing the integration in Eq.(23).

Up to this point we have assumed that the distribution of the WOS potential $\tilde{V}$ is normal, $\mathbb{P}(\tilde{V})$ given by Eq.(19) with a known noise σ^2. Ceperley and Dewing[37] discuss the practical issues using the penalty method. Following them, for a potential estimate using n WOS runners, we generate a sequence $\{\tilde{V}_0, \ldots, \tilde{V}_{n-1}\}$, where each $\tilde{V}_k$ is independent. We use $\tilde{V} = \sum_i \tilde{V}_i/n$ as the potential estimate, and $\chi^2 = \sum_i (\tilde{V}_i - \tilde{V})^2/n(n-1)$ as the estimator for the noise σ^2. Their suggested form for the correction to the noise when the distribution is not normal is

$$\frac{\sigma^2\tau^2}{2} \longrightarrow \frac{\chi^2\tau^2}{2} + \frac{\chi^4\tau^4}{4n(n+1)} + \frac{\chi^6\tau^6}{3(n+1)(n+3)} + \ldots \quad (24)$$

in Eq.(20).

We conclude this section by a comment on implementation. While constructing the propagator $G(\boldsymbol{R}, \boldsymbol{R}')$ it is customary to reuse the energy $E_L(\boldsymbol{R})$ which was calculated in a prior step during the move to the configuration $\boldsymbol{R}$. However, with the stochastic potential we need to reevaluate $\tilde{\mathbb{E}}_L(\boldsymbol{R})$ again, as otherwise this will introduce a bias.

VI. NUMERICAL TESTS

We demonstrate the techniques discussed in this paper in the context of a simple problem and calculate the polarizability of helium by placing a helium atom in the electric field generated between the plates of an infinite capacitor. This will illustrate several features of implementing the WOS algorithm. Alternatively, we can
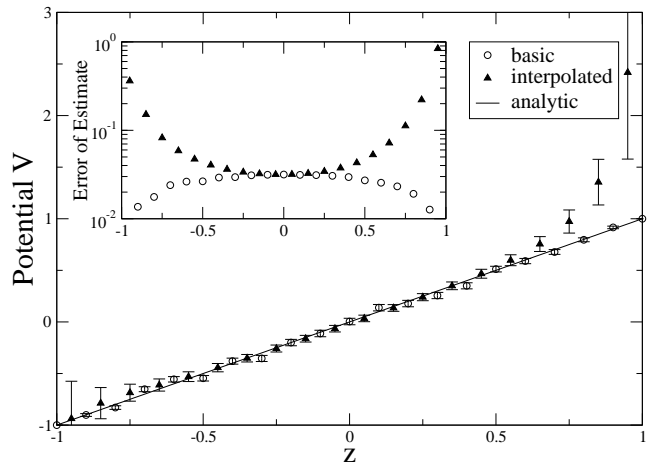
FIG. 3: A comparison of different WOS algorithms to evaluate the potential between the plates of an infinite capacitor. The circles represent the basic WOS calculation where each run is started from the point where the potential is sought. The triangles are the interpolated estimates from runners starting from the center. The line represents the exact analytic form of the potential. The inset shows a comparison of the errors from the different schemes. Each estimate involved 10^3 runners.

model the system by a constant electric field and compare the accuracy of quantum Monte Carlo using the stochastically estimated potential. The model potential neglects the effect of induced image charges which is small when the plates are far apart, but the WOS solution includes these corrections. We first describe the device, and compare the efficiency and accuracy of different refinements of the basic WOS algorithm to estimate the potential profile within the device.

A. Estimating the potential profile by different WOS refinements

The vertical plates of the capacitor are at a distance $z_L = \pm 1$, and plate voltages of $\Phi_{\text{app}} = \pm 1$ in arbitrary units (units will not be important until we start the quantum Monte Carlo calculations). We first test our methods of obtaining the potential profile of this device and compare with the analytic result.

The calculations are compared in Fig.(3). The circles represent the calculations of the basic WOS, where the potential at any point $P(\boldsymbol{r})$ is obtained by generating runs starting from that point. Since all the runs are computationally similar, the corresponding errors are also similar, as seen from the large plateau in the inset. As we approach either side of the z-axis, i.e. near the plates of the capacitor, the errors are reduced considerably since the relative proximity of one plate increases its influence, hence reducing the variance. This is seen from the plateau falling off near the sides.

The triangles are estimates from runs all of which originate from the same point ($z_0 = 0$), and use the interpola-

tion scheme described in section IV. Near the center this approach does just as well as the basic approach, as seen from the two curves in the inset coinciding. But further out near the plates the interpolation becomes worse as discussed earlier, since the entire estimate becomes dominated by only a few walks. The point is that while the basic WOS employed 10^3 runners for each of the 20 points in the plot, the interpolated method used 10^3 runners for the entire plot, hence it was about 20 times faster. In the calculations for the helium atom we expect even the polarized atom to remain well confined in the central region, and hence this approach will be three times faster (total number of particles being three) than the basic method.

We also implemented the other methods mentioned earlier, namely that of using antithetic variates and that of using a reference value with the correlated sampling. As expected antithetic variates did not show significant improvement. Also as expected, the use of correlated sampling using the reference value was greatly effective in speeding up the calculation about three times (the number of particles). This also holds considerable promise for more complicated geometries.

B. Importance Sampling

Importance sampling can be illustrated for this example of an infinite capacitor. As shown in section , the optimal importance function is the potential itself. Since the external potential in a capacitor is simply $\Phi(\boldsymbol{r}) = z$, this can be implemented to illustrate the construction of such functions. This can also be derived more graphically, by noting that what we want is an importance function that leads to sampling regions of the spheres preferentially in the z direction so that the walks are directed towards the capacitor plates and hence end quickly.

The actual algorithm employing this importance function is simple to describe. Consider the k-th domain $\mathcal{D}_k$ centered at $\boldsymbol{r}_k(x_k, y_k, z_k)$ and radius d_k, and $\boldsymbol{r}_{k+1}$ is the next point in the walk sampled on $\partial \mathcal{D}_k$ the domain surface. So the optimal importance function is

$$\frac{I(\boldsymbol{r}_{k+1})}{I(\boldsymbol{r}_k)} = \frac{\Phi(\boldsymbol{r}_{k+1})}{\Phi(\boldsymbol{r}_k)} = \frac{z_{k+1}}{z_k} = 1 + \frac{d_k}{z_k} \cos\theta_{k+1}$$

where θ_{k+1} is the angle between the $z = 0$ plane and the line joining $\boldsymbol{r}_k$ and $\boldsymbol{r}_{k+1}$. The sampling just depends on the cöordinate of the point we are about to sample $\boldsymbol{r}_{k+1}$, the cöordinates of the present point $\boldsymbol{r}_k$ are already known. Note that the optimal importance function weighted kernel is normalized.

We implement this algorithm on the computer and obtain zero variance as expected. One point to note is that the variance is limited to a small non-zero number due to the finiteness of the skin depth δ which can be made arbitrarily small. A better approach is simply to switch the shape of the domain near the boundary, or easier still, to discretize the region near the boundary into a grid, and a
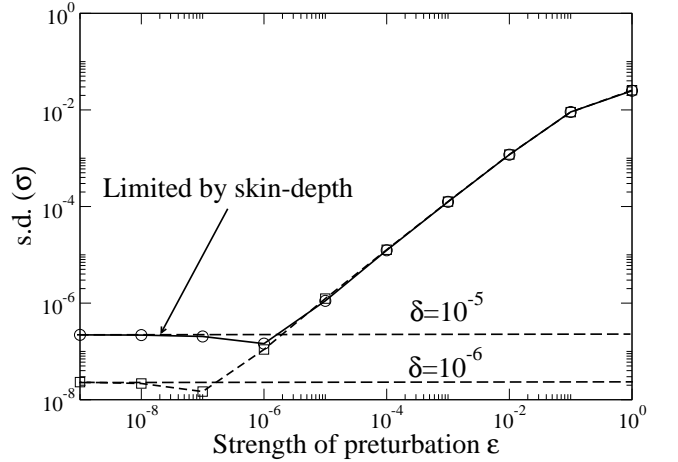

FIG. 4: As the non-optimal importance function approaches the optimal form, variance is reduced. For an algorithm using only spherical domains the variance approaches a limiting value due to the finite size of the skin-depth δ. Discretizing near the boundary will eliminate this limit.

discrete equivalent of WOS will exactly converge on the boundary and hence yield a zero variance.

Next we consider a small perturbation to the optimal importance function, $I(z) = z + \epsilon z^2$, $(\epsilon \ll 1)$i.e. we mix in a small quadratic term.

$$\frac{I(\boldsymbol{r}_{k+1})}{I(\boldsymbol{r}_k)} = \frac{z_{k+1} + \epsilon z_{k+1}^2}{z_k + \epsilon z_k^2}$$

This leads to an importance function quadratic in $\cos\theta_{k+1}$. The non-optimal importance function weighted kernel however is not normalized and we have to carry that in the weight. In Fig.(4) we show the result of the calculation. We plot the result with two values of skin depth δ and show that the error can indeed be arbitrarily reduced by reducing δ.

This generalizes to problems with more complicated geometries in a straightforward way. The optimal importance function is the potential itself, and for that one, the normalization of the importance-weighted kernel is unity. Hence for the general problem, one possibility is to utilize an approximate potential as the importance function. This approximate solution could be obtained in any number of ways including a finite element solution of the Poisson problem on a discretized grid using an approximate electron density. The solution, its gradient and Laplacian could be tabulated on the same mesh to generate a non-uniform distribution over a domain. To obtain the correct potential at the domain center, one would need to evaluate the approximate normalization over the domain surface and sample accordingly. Thus importance sampling would greatly improve the efficiency of the algorithm.

C. Polarizability of He by QMC

We implement these techniques to measure the polarizability of helium, and compare the results with that obtained by using a model potential. The polarization (estimated by $\langle z \rangle$) is not an observable of the Hamiltonian, and so we have to use the mixed estimator

$$p \equiv \langle z \rangle = 2\langle z \rangle_{DMC} - \langle z \rangle_{VMC}$$

This clearly is not the best way to measure polarizability since this increases the variance of the estimate. If the variance of the VMC and DMC calculations are σ_V^2 and σ_D^2 respectively then the variance of p is $(\sigma_V^2 + 4\sigma_D^2)^{1/2}$. Caffarel et al uses the Laplace transform of a two- (imaginary) time correlation function for a more accurate estimate of the polarization by quantum Monte Carlo[38]. Nevertheless, this simple approach will be able to investigate the main goal of this test, i.e. how the calculations using the WOS potential compare with those using the model potential.

We place a helium atom between the plates of an infinite capacitor. The plates are at $z_L = \pm 10$ a.u. and the helium atom is placed at $z_0 = 0$. A voltage of $\pm\Phi_{\mathrm{app}}$ is applied to the gates, and this is compared with a model electric field of $\mathcal{E}_z = -\Phi_{\mathrm{app}}/z_L$. All numbers are in atomic units. The plates are kept sufficiently far away from the atom such that the effect of the images charges induced in the plates is small. This allows a comparison of results obtained with WOS with that using a model linear potential $-\mathcal{E}_z z$. Also if the plates are very close to the atom it could interfere with the electron cloud and distort the atom radically.

We choose a trial wave-function of the form

$$\Psi_T(\boldsymbol{q}_1, \boldsymbol{q}_2) = |\mathbf{1}s(\boldsymbol{q}_1)\rangle|\mathbf{1}s(\boldsymbol{q}_2)\rangle \exp\left(-\frac{aq_{12}}{1 + bq_{12}}\right)$$

where the $\boldsymbol{q}$s are the electron coordinates, $q_{ij} = |\boldsymbol{q}_i - \boldsymbol{q}_j|$, and a and b are variational parameters. We can determine a to be $-1/2$ by imposing the cusp condition[2] which reflects the divergence in the wave-function when the two electrons approach each other. Here $|\mathbf{1}s(\boldsymbol{q})\rangle$ is the single particle orbital and same for up and down spins. This simple two electron problem avoids the complications of nodes in wave-functions and helps illustrate the main issues of using WOS with quantum Monte Carlo.

The conditions of the problem have been set such that the capacitor adds only a small perturbation to the helium atom, and thus we need only modify the single particle orbitals very slightly to reflect the polarization of the atom in the z direction. The wave-function of helium in free space is spherically symmetric, and since variational Monte Carlo does not modify the wave-function it would not be able to polarize the atom. Hence we introduce a parameter α which would control the polarization of the atom. A zero value of α would correspond to the
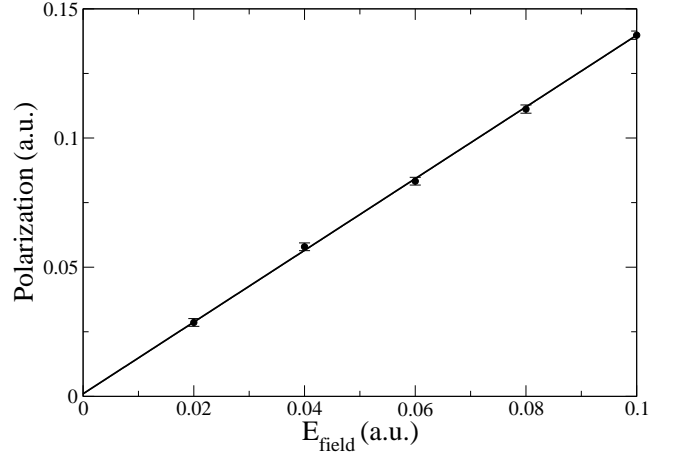

FIG. 5: Least square fit of the polarization data obtained from the WOS calculation of the helium atom placed between the plates of an infinite capacitor. The result used is the mixed estimator obtained from the VMC and DMC data presented in Table I. The data for the model calculation is not shown since it nearly overlaps with the WOS data.

unpolarized case. We choose a form

$$|\mathbf{1}s(\boldsymbol{q})\rangle = (1 + \alpha q_z) \sum_{j=0}^{4} c_j \exp(-\lambda_j q),$$

where q_z is the z-coordinate of $\boldsymbol{q}$, and the parameters c_j, λ_js are obtained from calculations of Clementi and Roetti[39]. We use pre-optimized values of these parameters ($c_1 = 2.063076 \times 10^{-1}$, $c_2 = 2.2346 \times 10^{-1}$, $c_3 = 4.082 \times 10^{-2}$, $c_4 = -9.94 \times 10^{-3}$, $c_5 = 2.3 \times 10^{-3}$ and $\lambda_1 = 1.4171, \lambda_2 = 2.3768, \lambda_3 = 4.3963, \lambda_4 = 6.527, \lambda_5 = 7.9425$).

We optimize the Jastrow parameter b and the polarization parameter α by correlated sampling. When we use the stochastic potential we minimize only the mean of the local energy, and not any combination of the variance. As described before, we record not only the configurations $\{\boldsymbol{R}\}$, but also the local potential energy $V(\boldsymbol{R}_m) \ \forall \ m$ for use in minimization of the variational energy. The polarization obtained from variational Monte Carlo with the optimized parameters provide an estimate for the polarization, but as noted earlier this is not very accurate since polarization is not an observable of the Hamiltonian.

D. Polarizability Results and Analysis of the Penalty Method

We test our code by calculating the ground state energy of a helium atom, our result $-2.90361(9)$ a.u. compares well with the best known theoretical estimate of -2.903724377034119598 a.u.[40] and experimental value of -2.9038 a.u.[41]. Next we carry out the calculations in presence of an electric field by two different methods as described before. WOS refers to the calculations using

the stochastic potential, and "model" refers to the linear potential model. The results are shown in Table I. From a least-square fit of the data our estimate for the polarization is 1.417(16) a.u. from the WOS data as in Fig.(5) and 1.362(16) a.u. from the model calculation, which can be compared with 1.382(16) a.u. as obtained by Cafarrel et al.[38].

The result suffers from the drawbacks of our estimator as discussed before, but the main point to note is the comparison between the WOS and "model" results. The difference in the result comes from the induced charges in the capacitor (not captured in the model) as will be discussed below. From Table I we see that the results agree within error-bars for both the optimized VMC calculations and DMC. The diffusion Monte Carlo calculations were carried out using only twenty runners for each walker configuration. We also use the penalty method the results of which will be discussed next.

To investigate the effect of using the WOS potential in diffusion Monte Carlo we study the time-step error, since we expect the effect of the using the stochastic potential to be magnified with increasing time-step, as seen in Eq.(17). In Fig.(6) we compare the DMC ground state energy from the model potential calculation to that using WOS for different number of runners (per walker). The uppermost curve labeled "model" is the linear potential model which shows a quadratic scaling with the time-step. The lowermost curve labeled WOS(1) represents DMC calculations using a single runner (per walker) without any penalty correction. This obviously suffers from the branching error which is magnified at larger time-steps.

| | E_G | | | | p_z | | | | | |
| | VMC | | DMC | | VMC | | DMC | | Mixed | |
$\mathcal{E}_z$	WOS	model	WOS	model	WOS	model	WOS	model	WOS	model
0.02	-2.888461(92)	-2.888080(97)	-2.904313(85)	-2.904149(89)	0.0268(6)	0.0257(6)	0.0277(7)	0.0277(7)	0.0286(15)	0.0297(15)
0.04	-2.889087(95)	-2.888904(93)	-2.905298(82)	-2.904932(82)	0.0611(6)	0.0469(6)	0.0595(6)	0.0529(6)	0.0579(15)	0.0589(15)
0.06	-2.890392(100)	-2.890119(94)	-2.906741(87)	-2.906314(81)	0.0827(6)	0.0702(7)	0.0830(7)	0.0776(7)	0.0833(15)	0.0850(16)
0.08	-2.892102(100)	-2.891927(99)	-2.908636(84)	-2.908208(86)	0.1084(7)	0.1081(7)	0.1098(7)	0.1109(7)	0.1112(16)	0.1137(16)
0.10	-2.894533(110)	-2.894134(95)	-2.911209(89)	-2.910856(89)	0.1332(7)	0.1332(7)	0.1385(7)	0.1341(7)	0.1438(16)	0.1350(16)

TABLE I: Calculation of polarization of helium with quantum Monte Carlo. The system consists of a helium atom placed between the plates of an infinite capacitor as described in this section. Two similar calculations were run, one using the stochastic potential using the WOS algorithm, and the other using a model linear potential. The variational Monte Carlo results here are obtained by optimizing the trial wave-function. For DMC, we used a time-step of $\tau = 0.01$.

If however we increase the number of runners (per walker) to 5, we see from the WOS(5) curve that the result is improved but still suffers from the bias. The use of the penalty method corrects this problem, and the curve marked penalty(5) follows the model potential for the entire range of τ that we tested. We also note that the correction of Eq.(24) did not make a difference to the calculation within the given error-bars. If we increase the number of runners to about twenty, then the basic WOS calculation without the penalty method is greatly improved, and it overlaps with the correct result for a large range of τ up to about 0.2 in this calculation; but beyond that the bias in the result becomes apparent. Since the calculations using the penalty method with five runners and twenty runners (per walker) overlapped with each other we did not show them separately in the figure.

Though the model and the penalty calculations run parallel, they are offset by a constant amount. This is to be expected since the model calculation neglects the effect of the charges induced on the capacitor plates. A very simple calculation using dipole images (but neglecting multiple reflections) estimates this effect to be about 2×10^{-4} a.u., the same order of the observed shift of 3×10^{-4} a.u. Thus the WOS calculation can capture the induced charge effect neglected by the model.

To study the effect of the penalty method, we compare in Fig.(7) the effect of the two different types of penalty corrections that we discussed in section V B. In the calculations we use a large number of runners (per walker) to estimate the potential to be used in the branching term. The first estimator uses a separately sampled value, we call this the uncorrelated penalty approach. We can construct another estimator using the same estimate that we use for the branching, but then we have to add another correction to it as discussed before. Fig.(7) shows that the uncorrelated penalty method has a faster convergence, but both approaches converge for large number of runners (per walker).

Also shown in Fig.(7) is the estimate of the model calculation. We see that the WOS calculations converge to
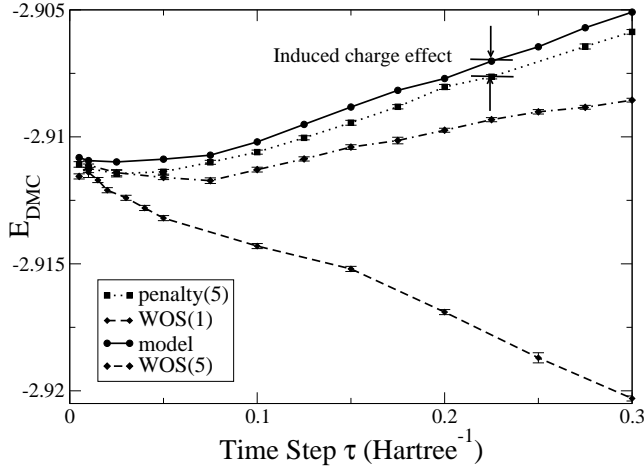
FIG. 6: Ground state DMC energy of the helium atom in an electric field of $\mathcal{E}_z = 0.1$ for different time steps. In parenthesis is the number of runners used per walker for the WOS calculations. This is compared with the calculation using the model field.
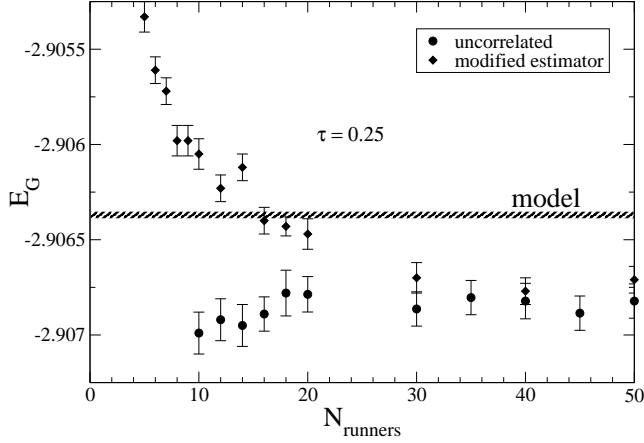

FIG. 7: Testing the convergence of the two penalties. The uncorrelated penalty method using an independent uncorrelated (to the branching) potential estimate converges much faster than the approach where we modify the estimator. However, for a large number of runners the second converges to the correct result from above. The calculation was carried out at $\tau = 0.25$. The difference from the model is due to the induced charge effect.

a value lower than the model. This is the induced charge effect as mentioned earlier. As we increase the separation of the capacitor plates, this effect decreases and for a plate separation of about 100 a.u. (keeping the electric field constant) the WOS results converge to the model value. This demonstrates another important feature of the algorithm. In order to keep the field constant, we had to increase the gate voltages. The algorithm remained

stable under this scaling.

The WOS calculations with a single runner (per walker) were only about four times slower than that with the model potential, this is not too bad considering the generality of the WOS method. The WOS method can be applied to any complicated geometry for which a model might not exist, however the time taken by the code will also depend on the complexity of the device geometry. These calculations scale linearly with the number of runners, for instance the calculation with twenty runners was about twenty times more expensive than the one with a single runner.

VII. CONCLUSIONS

We have demonstrated that a stochastically obtained potential can be used efficiently with popular quantum Monte Carlo methods, specifically variational and diffusion Monte Carlo. To this end we have modified and improved an efficient "Walk On Spheres" algorithm which can handle arbitrary device geometries and gate voltages and even take care of induced charge effects of the evolving walker configurations. This approach will make possible accurate application of quantum Monte Carlo to realistic models of physical devices.

We also demonstrated the application of the penalty method to account for the stochastic nature of the potential. To use it with diffusion Monte Carlo we needed to modify the branching term and use a potential estimate which had to be uncorrelated with the estimator.

The future goals involve applying this method to more complicated devices like quantum dots in semiconductor heterostructures. Also of interest is to extend this method with other quantum Monte Carlo methods like reptation and domain Green's function Monte Carlo.

[1] Ceperley D. M., Reviews of Modern Physics **71**, S438 (1999).

[2] Foulkes W. M. C, Mitas L., Needs R. J., and Rajagopal G., Reviews of Modern Physics **73**, 33 (2001).

[3] Hammond B. L., Lester W. A. Jr., and Reynolds P. J., *Monte Carlo Methods in Ab Intio Quantum Chemistry*, vol. 1 (World Scientific, 1994).

[4] Fahy S., Wang X. W., and Louie S. G., Physical Review Letters **61**, 1631 (1988).

[5] Ceperley D. M. and Alder B. J., Journal de Physique **C7**, 295 (1980).

[6] Moroni S., Ceperley D. M., and Senatore G., Physical Review Letters **75**, 689 (1995).

[7] Ceperley D. M. and Alder B. J., Physica **108B**, 875 (1981).

[8] Natoli V., Martin R. M., and Ceperley D. M., Physical Review Letters **70**, 1952 (1993).

[9] Grossman J. C. and Mitas L., Physical Review Letters **74**, 1323 (1995).

[10] Ashoori R. C., Nature **379**, 413 (1996).

[11] Petroff P. M., Gossard A. C., Logan R. A., and Wiegmann W., Applied Physics Letters **41**, 635 (1982).

[12] Kastner M. A., Review of Modern Physics **64**, 849 (1992).

[13] Harrison Paul, *Quantum Wells, Wires and Dots* (John Wiley and Sons Ltd., 1999).

[14] Rontani M., Rossi F., Manghi F., and Molinari F., Physical Review B **59**, 10165 (1999).

[15] Matagne P., Wilkens T., Leburton J. P., and Martin R. M., Proceedings of the 8th International Workshop on Computational Electronics (ICWE-8), Journal of Computational Electronics **1**, 135 (2002).

[16] Ceperley D. M., Chester G. V., and Kalos M. H., Physical Review B **16**, 3081 (1977).

[17] Hirose K. and Wingreen N. S., Physical Review B **59**, 4604 (1999).

[18] Koskinen M., Manninen M., and Reimann S. M., Physical Review Letters **79**, 1389 (1997).

[19] Kakutani S., Proc. Imp. Acad. (Tokyo) **20**, 706 (1944).

[20] Metropolis N. and Ulam S., Journal of American Statistical Associaton **44**, 335 (1949).

[21] Muller M. E., Annals of Mathematical Statistics **27**, 567 (1956).

[22] Haji-Sheikh A. and Sparrow E. M., Journal of Heat Transfer **C89**, 121 (1967).

[23] Bevensee R. M., Proceedings of IEEE **61**, 423 (1973).

[24] Beasley M. D. R., Pickles J. H., d'Amico G., and et. al., Proceedings of IEE **126**, 126 (1979).

[25] Zachmanoglou E. C. and Thoe D. W., *Introduction to Partial Differential Equations with Applications* (Dover Publications, Inc., 1976).

[26] Jackson J. D., *Classical Electrodynamics* (John Wiley and Co., 1974), 2nd ed., pp 44, Eq.(1.44).

[27] Kalos M. H., Levesque D., and Verlet L., Physical Review A **9**, 2178 (1974).

[28] DeLaurentis J. M. and Romero L. A., Journal of Computational Physics **90**, 123 (1990).

[29] Pickles J. H., Proceedings of IEE **124**, 1271 (1977).

[30] Jackson J. D., *Classical Electrodynamics* (John Wiley and Co., 1974), 2nd ed., pp 56.

[31] Filippi C. and Umrigar C. J., arXiv:cond-mat/991132v1 (1999).

[32] Umrigar C. J., Wilson K. G., and Wilkins J. W., Physical Review Letters **60**, 1719 (1988).

[33] Kalos Malvin H. and Whitlock Paula A., *Monte Carlo Methods*, vol. I: Basics (John Wiley & Sons, 1986).

[34] Metropolis N., Rosenbluth A. W., Rosenbluth M. N., Teller A. H., and Teller E., Journal of Chemical Physics **21**, 1087 (1953).

[35] Umrigar C. J., Nightingale M. P., and Runge K. J., Journal of Chemical Physics **99**, 2865 (1993).

[36] Reynolds P. J., Ceperley D. M., Alder B. J., and Lester W. A., Journal of Chemical Physics **77**, 5593 (1982).

[37] Ceperley D. M. and Dewing M., Journal of Chemical Physics **10**, 9812 (1999).

[38] Caffarel M., Rerat M., and Pouchan C., Physical Review A **47**, 3704 (1993).

[39] Clementi E. and Roetti C., Atomic Data and Nuclear Data Tables **14**, 177 (1977).

[40] Hagstrom S. A. and Sims J. S., The International Journal of Quantum Chemistry. (2002).

[41] Veillard A. and Clementi E., Journal of Chemical Physics **49**, 2415 (1968).